deficiency would decrease atherothrombotic tendency.

Previous reports of apoC-III deficiency in humans were complicated by the prothrombotic effects of accompanying apoA-I and/or apoA-IV deficiency (*27*–*30*), small sample sizes and/or structurally abnormal apoC-III (*31*, *32*). The current report of a favorable lipid profile and reduced subclinical coronary artery atherosclerosis in R19X null mutation carriers provides strong evidence in a relatively large number of individuals that apoC-III deficiency (by ~50% of normal levels) is indeed cardioprotective.

Indirectly lowered *APOC3* expression is one mechanism of the lipid-lowering effect of fibrates (*33*), and the use of several other lipid-lowering agents, including statins, thiazolidinediones, ezetimibe, niacin, fish oil, and weight loss, has also been associated with decreases in apoC-III levels [reviewed in (*20*)]. That a naturally occurring null mutation in *APOC3* confers a favorable lipid profile and apparent cardioprotection and does not result in any obvious detrimental effect raises the possibility that therapies aimed specifically at down-regulating apoC-III expression will be clinically efficacious and safe in reducing the morbidity and mortality associated with CHD.

References and Notes

1. J. L. Goldstein, H. G. Schrott, W. R. Hazzard, E. L. Bierman, A. G. Motulsky, *J. Clin. Invest.* **52**, 1544 (1973).
2. N. Sarwar *et al.*, *Circulation* **115**, 450 (2007).
3. M. Miller *et al.*, *J. Am. Coll. Cardiol.* **51**, 724 (2008).
4. J. C. Cohen, E. Boerwinkle, T. H. Mosley Jr., H. H. Hobbs, *N. Engl. J. Med.* **354**, 1264 (2006).
5. S. Bansal *et al.*, *JAMA* **298**, 309 (2007).
6. B. G. Nordestgaard, M. Benn, P. Schnohr, A. Tybjaerg-Hansen, *JAMA* **298**, 299 (2007).
7. B. D. Mitchell *et al.*, *Am. Heart J.* **155**, 823 (2008).
8. Materials and methods are available as supporting material on *Science* Online.
9. J. P. Kane, R. J. Havel, in *The Online Metabolic and Molecular Bases of Inherited Diseases (OMMBID)* (McGraw-Hill, New York, ed. 8, 2001), chap. 114.
10. N. Maeda *et al.*, *J. Biol. Chem.* **269**, 23610 (1994).
11. A. V. Hospattankar, H. B. Brewer Jr., R. Ronan, T. Fairwell, *FEBS Lett.* **197**, 67 (1986).
12. O. Isken, L. E. Maquat, *Genes Dev.* **21**, 1833 (2007).
13. E. Nagy, L. E. Maquat, *Trends Biochem. Sci.* **23**, 198 (1998).
14. W. Post *et al.*, *Circulation* **115**, 717 (2007).
15. Expert Panel on Detection, Evaluation, and Treatment of High Blood Cholesterol in Adults, *JAMA* **285**, 2486 (2001).
16. P. W. Wilson *et al.*, *Circulation* **97**, 1837 (1998).
17. R. Detrano *et al.*, *N. Engl. J. Med.* **358**, 1336 (2008).
18. R. L. McClelland, H. Chung, R. Detrano, W. Post, R. A. Kronmal, *Circulation* **113**, 30 (2006).
19. A. R. Folsom *et al.*, *Arch. Intern. Med.* **168**, 1333 (2008).
20. E. M. Ooi, P. H. Barrett, D. C. Chan, G. F. Watts, *Clin. Sci. (Lond.)* **114**, 611 (2008).
21. H. N. Ginsberg *et al.*, *J. Clin. Invest.* **78**, 1287 (1986).
22. V. Clavey, S. Lestavel-Delattre, C. Copin, J. M. Bard, J. C. Fruchart, *Arterioscler. Thromb. Vasc. Biol.* **15**, 963 (1995).
23. D. C. Chan, M. N. Nguyen, G. F. Watts, P. H. Barrett, *J. Clin. Endocrinol. Metab.* **93**, 557 (2008).
24. A. Kawakami *et al.*, *Circulation* **113**, 691 (2006).
25. P. Libby, *Circ. Res.* **100**, 299 (2007).
26. F. M. Sacks *et al.*, *Circulation* **102**, 1886 (2000).
27. R. A. Norum *et al.*, *N. Engl. J. Med.* **306**, 1513 (1982).
28. S. K. Karathanasis, R. A. Norum, V. I. Zannis, J. L. Breslow, *Nature* **301**, 718 (1983).
29. S. K. Karathanasis, E. Ferris, I. A. Haddad, *Proc. Natl. Acad. Sci. U.S.A.* **84**, 7198 (1987).
30. J. M. Ordovas, D. K. Cassidy, F. Civeira, C. L. Bisgaier, E. J. Schaefer, *J. Biol. Chem.* **264**, 16339 (1989).
31. A. von Eckardstein *et al.*, *J. Clin. Invest.* **87**, 1724 (1991).
32. H. Liu *et al.*, *J. Lipid Res.* **41**, 1760 (2000).
33. J. Auwerx, K. Schoonjans, J. C. Fruchart, B. Staels, *Atherosclerosis* **124** (suppl.), S29 (1996).

34. We gratefully acknowledge our Amish liaisons, field workers, and clinic staff and the extraordinary cooperation and support of the Amish community, without which these studies would not have been possible. We thank R. Agarwala and A. Schäffer for assistance in pedigree construction and K. Ryan for data management. This work was supported by NIH grants R01 HL088119, R01 AR046838, U01 HL72515, R01 AG18728, and U01 HL084756; General Clinical Research Centers Program, National Center for Research Resources (NCRR), NIH; the University of Maryland General Clinical Research Center, grant M01 RR 16500; University of Maryland Clinical Nutrition Research Unit grant P30 DK072488; the Johns Hopkins University General Clinical Research Center, grant M01 RR 000052; the Baltimore Veterans Administration Geriatric Research and Education Clinical Center (GRECC); and the Paul Beeson Faculty Scholars in Aging Program.

Supporting Online Material

www.sciencemag.org/cgi/content/full/322/5908/1702/DC1
Materials and Methods
SOM Text
Figs. S1 to S8
Tables S1 to S5
References

9 June 2008; accepted 31 October 2008
10.1126/science.1161524

Regulation of Dendritic Cell Migration by CD74, the MHC Class II–Associated Invariant Chain

Gabrielle Faure-André,[1]* Pablo Vargas,[1,2]* Maria-Isabel Yuseff,[1] Mélina Heuzé,[1] Jheimmy Diaz,[1] Danielle Lankar,[1] Veronica Steri,[1] Jeremy Manry,[1] Stéphanie Hugues,[1] Fulvia Vascotto,[1] Jérôme Boulanger,[3] Graça Raposo,[3] Maria-Rosa Bono,[2,4] Mario Rosemblatt,[2,4,5] Matthieu Piel,[3]† Ana-Maria Lennon-Duménil[1]†

Dendritic cells (DCs) sample peripheral tissues of the body in search of antigens to present to T cells. This requires two processes, antigen processing and cell motility, originally thought to occur independently. We found that the major histocompatibility complex II–associated invariant chain (Ii or CD74), a known regulator of antigen processing, negatively regulates DC motility in vivo. By using microfabricated channels to mimic the confined environment of peripheral tissues, we found that wild-type DCs alternate between high and low motility, whereas Ii-deficient cells moved in a faster and more uniform manner. The regulation of cell motility by Ii depended on the actin-based motor protein myosin II. Coupling antigen processing and cell motility may enable DCs to more efficiently detect and process antigens within a defined space.

Dendritic cells (DCs) patrol the body periphery by efficiently moving across tissues while retaining a high capacity for antigen (Ag) internalization. Ags are internalized into endosomes, degraded into peptides that are loaded onto major histocompatibility complex (MHC) molecules, and subsequently exposed at the cell surface of DCs (*1*). If DCs detect an Ag-associated activating signal, they enter into a maturation program that comprises an increase followed by a complete arrest of macropinocytosis and phagocytosis, maximizing uptake and processing of the activating Ag (*2*–*4*), as well as the modification of their migratory properties, enabling them to home to secondary lymphoid organs and present the resulting peptide-MHC complexes to T cells (*5*). Ag uptake and processing and cell migration must therefore be coordinated for DCs to efficiently activate T lymphocytes, suggesting that common regulatory mechanisms are involved. Although little is known about DC locomotion, it was recently shown that DCs move in the interstitial spaces of tissues by using amoeboid-like migration, which requires actomyosin contractility but not integrin-mediated adhesion (*6*).

Several lines of evidence point to the MHCII-associated protein invariant chain (Ii or CD74) as a good candidate to regulate DC migration. Indeed, beyond its key role in MHCII trafficking and peptide loading, Ii was shown to associate with two actin-interacting proteins known to regulate cell locomotion: the motor protein myosin II, which controls actomyosin contractility, and the adhesion molecule CD44 (*7*–*9*). To investigate whether Ii regulates DC migration, we compared the in vivo migratory properties of wild-type (WT) and $Ii^{-/-}$ DCs (fig. S1A). Bone marrow–derived DCs (BM-DCs) were

[1]INSERM U653, Institut Curie, 12 rue Lhomond, 75005, Paris, France. [2]Departamento de Biología, Facultad de Ciencias, Universidad de Chile, Las Palmeras 3425, Santiago, Chile. [3]CNRS UMR144, Institut Curie, 12 rue Lhomond, 75005, Paris, France. [4]Fundación Ciencia para la Vida and Instituto Milenio de Biología Fundamental y Aplicada, Avenida Zañartu 1482, Santiago, Chile. [5]Facultad de Ciencias de la Salud, Universidad Andrés Bello, Avenida Zañartu 1482, Santiago, Chile.

*These authors contributed equally to this work.
†To whom correspondence should be addressed. E-mail: amlennon@curie.fr (A.-M.L.-D.) and mpiel@curie.fr (M.P.)

loaded with fluorescent dyes [in the presence of lipopolysaccharide (LPS) to induce CCR7 expression] and transferred into the footpad of C57/BL6 mice, and their arrival at the draining lymph node (DLN) was monitored 48 hours after transfer. Increased numbers of Ii-deficient DCs compared with WT cells were found in the DLN of recipient mice (Fig. 1A and fig. S2A). Fluorescein isothiocyanate (FITC)–painting experiments of the ear also showed that enhanced numbers of endogenous DCs had reached the DLN in $Ii^{-/-}$ mice after 24 hours compared with the numbers in WT mice (Fig. 1B). This difference did not result from passive diffusion of FITC because $Ii^{+/+}$ and $Ii^{-/-}$ mice displayed similar numbers of DCs in LNs at the steady state (fig. S2B). Thus, the absence of Ii facilitates the accumulation in LNs of activated DCs that migrate from the periphery.

Cathepsin S cleaves the cytosolic tail of Ii when MHCII-Ii complexes have reached endolysosomes. This is required for peptide loading onto MHCII and transport of MHCII-peptide complexes to the cell surface (*10*, *11*). In the absence of CatS, MHCII-Ii complexes accumulate in endolysosomes and, to a minor extent, at the plasma membrane (*12*). We analyzed the migratory capacity of $CatS^{-/-}$ DCs, which display enhanced Ii protein levels (fig. S1, A to C) (*10*–*12*). $CatS^{-/-}$ DCs transferred into the footpad of C57/BL6 mice migrated less efficiently from the periphery to LNs than did WT DCs (Fig. 1C). Increased numbers of transferred $CatS^{-/-}$ DCs compared with WT cells were found in the footpad, suggesting that $CatS^{-/-}$ DCs remained at the injection site rather than

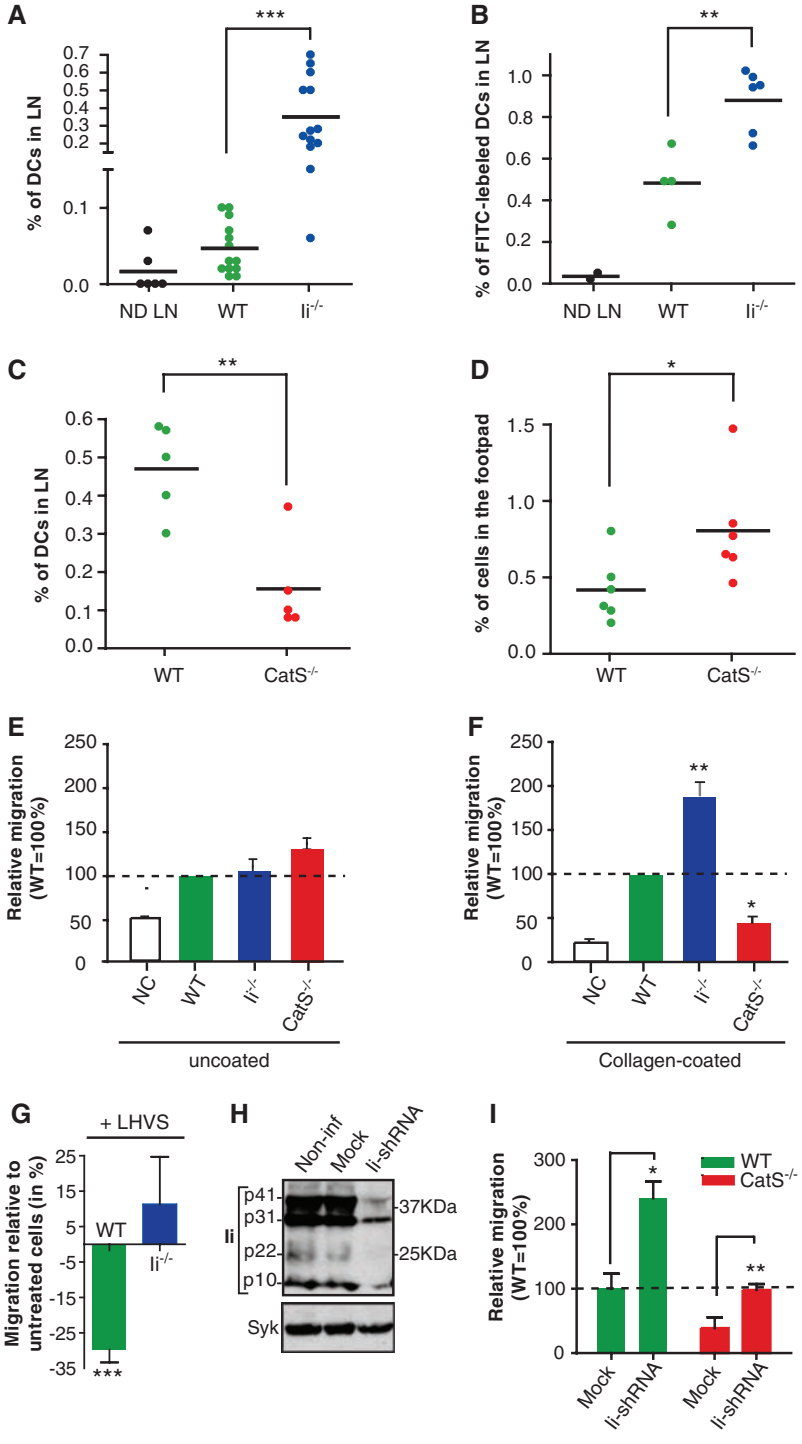

Fig. 1. Ii negatively regulates DC migration in vivo and in collagen-coated transwells. (**A**) Fluorescently labeled WT and $Ii^{-/-}$ DCs were coinjected into the footpad of C57BL/6 recipient mice. Draining and nondraining (ND) LNs were analyzed by flow cytometry after 48 hours. The presence of migrating DCs is displayed as a percentage of total LN cells (each dot represents one mouse, four independent experiments, ***$P < 0.0001$). (**B**) Ears from WT or $Ii^{-/-}$ were painted with a FITC-containing irritating solution. Twenty-four hours later, draining LNs were analyzed by flow cytometry (each dot represents one mouse, three independent experiments **$P = 0.004$). (**C**) Migration experiment of transferred WT and $CatS^{-/-}$ BM-DCs performed as described in (A). (**D**) The numbers of fluorescent DCs remaining in the footpad of recipient mice. For (C) and (D), results are from three independent experiments; **$P = 0.0034$; *$P = 0.0445$. (**E** and **F**) Migration of WT, $Ii^{-/-}$, and $CatS^{-/-}$ BM-DCs in uncoated (E) and collagen-coated (F) transwells toward CCL19 and CCL21 (NC, no chemokines). Results are expressed in percentage and normalized to migration of WT DCs (mean ± SD, three independent experiments, **$P = 0.001$, *$P = 0.01$). (**G**) Inhibition of DC migration by the CatS inhibitor LHVS, performed as in (F). The results are represented as the percentage of LHVS-treated DCs that migrated relative to untreated cells (mean ± SD, three independent experiments, ***$P = 0.0005$). (**H**) Ii depletion upon infection of day 4 BM-DCs with a lentivirus encoding an Ii shRNA. Infected BM-DCs were collected at day 10, lysed, and analyzed by immunoblotting for Ii and Syk expression. (**I**) Migration experiment of Ii-depleted BM-DCs performed as described in (F). The results are expressed in percentage and normalized to migration of control WT DCs (mean ± SD, two independent experiments, **$P = 0.005$, *$P = 0.05$).

homed to another tissue (Fig. 1D). Thus, enhanced levels of Ii in CatS$^{-/-}$ DCs correlate with reduced in vivo migration.

We next compared the ability of WT, Ii$^{-/-}$, and CatS$^{-/-}$ DCs to migrate toward a CCL19/CCL21 gradient in transwells. Ii-deficient cells migrated more efficiently than WT DCs, and CatS$^{-/-}$ cells showed impaired migration in collagen-coated but not in uncoated transwells (Fig. 1, E and F). Transfer of supernatants between WT, Ii$^{-/-}$ and CatS$^{-/-}$ DCs had no effect on cell migration, and Ii levels did not affect the capacity of DCs to degrade gelatin-FITC (fig. S3, A and B). Thus, down-regulation of DC migration by Ii results neither from altered response to CCL21 and CCL19 chemokines nor from differential secretion of soluble factors.

The specific CatS inhibitor LHVS (N-morpholinurea-homophenylalanyl-leucyl-vinylsulfonemethyl) significantly reduced the migration of WT DCs (Fig. 1G) (*13*). However, incubation of Ii-deficient DCs with LHVS did not compromise their migration (Fig. 1G). This result indicates that decreased migration of CatS$^{-/-}$ DCs resulted from Ii accumulation and not from an Ii-independent action of the protease. This observation was further strengthened by showing that short hairpin-mediated RNA interference (shRNA) depletion of Ii in CatS$^{-/-}$ DCs restored their ability to migrate in collagen-coated transwells (Fig. 1, H and I). Thus, Ii negatively regulates the capacity of DCs to move across a protein matrix in vitro and in vivo.

To unravel the mechanisms by which Ii regulates DC migration, we analyzed DC motility by time-lapse imaging with microfabricated 4-μm-diameter channels (*14*–*16*) (fig. S4). Nonactivated WT BM-DCs displayed an average median instantaneous velocity of 6.5 μm min^{-1} ± 3.4 (median ± SD) (Fig. 2A and movie S1). These values are compatible with the ones recently reported for BM-DC migrating in three-dimensional collagen matrices and in the mouse skin (*6*), validating microchannels as an adequate tool to study DC motility. Strikingly, 71% of Ii$^{-/-}$ DCs migrated at velocities above 6.5 μm min^{-1}, some of them reaching speeds two- to threefold higher (Fig. 2, A to C, and movie S2) ($P = 1.2 \times 10^{-6}$). On the contrary, the velocities of 76% of CatS$^{-/-}$ DCs fell below 6.5 μm min^{-1} (Fig. 2, A to C, and movie S3) ($P = 1.8 \times 10^{-3}$). Hence, Ii levels regulate the speed of DCs that migrate in a confined microenvironment, with Ii-deficiency favoring fast DC migration.

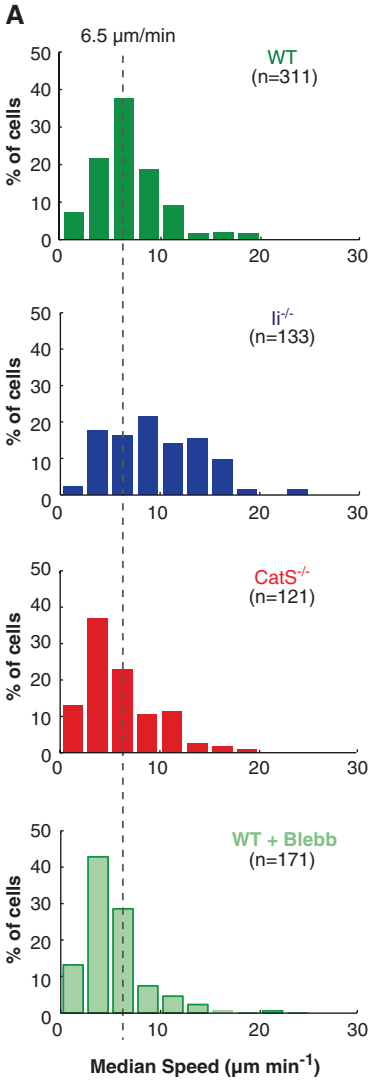

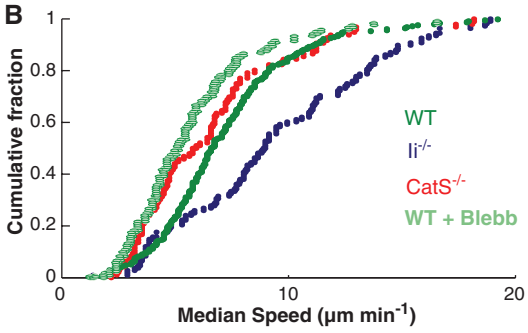

C

	p-value
WT vs Ii$^{-/-}$	1.24×10^{-6}
WT vs CatS$^{-/-}$	1.8×10^{-3}
WT vs WT + Blebb	2.6×10^{-6}
Ii$^{-/-}$ vs CatS$^{-/-}$	1.1×10^{-7}
Ii$^{-/-}$ vs WT + Blebb	8.6×10^{-13}
CatS$^{-/-}$ vs WT + Blebb	8×10^{-2}

Fig. 2. Ii decreases the velocity of DCs migrating in confining microchannels. (**A** and **B**) Distribution of median instantaneous speeds for Ii$^{-/-}$, CatS$^{-/-}$, and WT DCs treated with 20 μM blebbistatin. In (B), speed distribution is represented in a cumulative graph to allow statistical analysis. (**C**) Velocity distributions are significantly different from each other with a 95% confidence interval. Velocity distributions of CatS$^{-/-}$ and blebbistatin-treated DCs are not significantly different.

While imaging WT DCs migrating along microchannels, we noticed that most of the cells underwent important speed fluctuations during motion (Fig. 3A and movie S1). Two phases were observed: a motile phase during which pseudopods were extended at the cell front, leading to the formation of big vesicles (most likely macropinosomes), followed by a rather static phase during which these vesicles were transported backward (Fig. 3 and movie S4). Ii$^{-/-}$ DCs showed a more regular, continuous movement, and slow motility phases were rarely observed (Fig. 3A and movie S2). Even when comparing WT and Ii$^{-/-}$ DCs that displayed a similar median velocity, the speed fluctuations undergone by cells during migration were reduced in the absence of Ii (Fig. 3C). These results suggested that Ii regulates DC migration by inducing slowing-down phases during motion. Accordingly, when measuring the local speed variation of individual migrating DCs, we obtained values significantly lower for Ii-deficient cells compared with those of their WT counterpart, verifying that Ii$^{-/-}$ DCs undergo less velocity variation during motion (Fig. 3D) ($P = 7.6 \times 10^{-6}$). Furthermore, 50% of Ii$^{-/-}$ DCs spent most of their time (>80%) migrating faster than 6.5 μm min^{-1} (the WT median speed), whereas only 24% of WT DCs did so (fig. S6). These results indicate that Ii deficiency favors sustained DC migration at high speed. Thus, we conclude that Ii reduces DC migration by transiently slowing down DC velocity.

We next addressed the molecular mechanisms underlying the regulation of DC migration by Ii. Myosin II is required for DCs to migrate in collagen matrices and in vivo (*6*). Accordingly, we found that treatment of WT and Ii-deficient DCs with low concentrations of the myosin II inhibitor blebbistatin impaired their migration in collagen-coated transwells (fig. S7, A and B, and movie S5). In microchannels, the speed of WT DCs significantly decreased when inhibiting myosin II activity, with 76% of the cells migrating at velocities below 6.5 μm min^{-1} (WT median velocity, Fig. 2, A to C) ($P = 2.6 \times 10^{-7}$). Blebbistatin-treated DCs showed a velocity distribution similar to that of CatS$^{-/-}$ cells (Fig. 2, A to C) ($P = 8 \times 10^{-2}$), suggesting that myosin II activity might be compromised in CatS$^{-/-}$ DCs. In view of the ability of myosin II to interact with MHCII-Ii complexes in DCs (*7*), we hypothesized that Ii retention in CatS$^{-/-}$ DCs alters myosin II localization and activity.

To address this hypothesis, we analyzed myosin II and Ii distribution in CatS$^{-/-}$ DCs plated on rectangular fibronectin-coated micropatterns to obtain a spatial intracellular organization close to the one of elongated DCs migrating

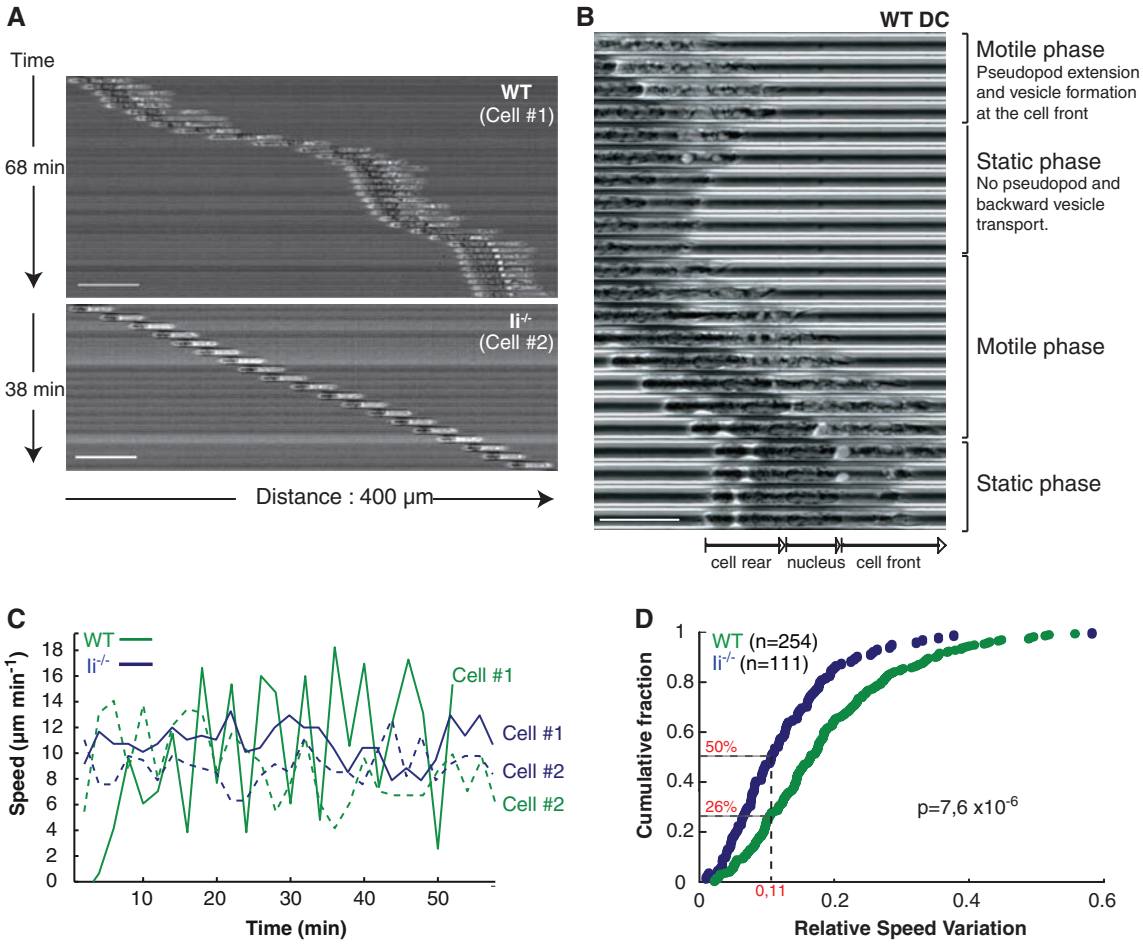

Fig. 3. Ii imposes a discontinuous migration mode to DCs. (**A**) DCs migrating along a 4-µm fibronectin-coated microchannel, covering a distance of 400 µm. Sequential images (10× objective phase) of temporal sequences were placed one below the other (vertical axis). The interval between two images is 2 min. Scale bar indicates 50 µm. (**B**) Sequential high resolution (100×) phase contrast images of a WT cell (movie S1) migrating along a microchannel. The channel part displayed is 88 µm long (vertical axis) with images taken over 14 min (40 s between each image, horizontal axis). Scale bar, 20 µm. (**C**) Representative examples of velocities displayed by individual WT and $Ii^{-/-}$ DCs as a function of time. The data were extracted from movies S1 and S2. WT cell number 1 and $Ii^{-/-}$ cell number 2 correspond to the DCs shown in (A). (**D**) Cumulative distribution of the relative speed variations of WT and $Ii^{-/-}$ DCs, calculated as the average of the local deviation from the local mean (two points before and two points after each time point) divided by the global median velocity.

along microchannels (fig. S8A). Ii-containing structures are known to accumulate in the perinuclear region of $CatS^{-/-}$ DCs (*12*). We observed an enrichment of myosin II heavy chain (MyoIIHC) in these structures (Fig. 4A) compared with a weaker colocalization with the more heterogeneous distribution of Ii in WT DCs, (Fig. 4A and fig. S8B). Equivalent results were obtained in WT cells treated with the CatS inhibitor LHVS (fig. S8B). Cryoimmunoelectron microscopy experiments confirmed the presence of myosin II light chain (MLC) in these enlarged endolysosomal compartments of $CatS^{-/-}$ DCs (Fig. 4B). Because these peculiar compartments form as a result of Ii retention in $CatS^{-/-}$ cells (*17*) and therefore have no structural equivalent to be compared with in WT DCs, it was not possible to provide a rigorous quantification for this qualitative difference. However, we rarely found MLC and Ii colocalizing in endolysosomes of WT DCs (fig. S8C). This result was further verified quantitatively by using biochemistry: The amounts of MyoIIHC and MLC (20 kD) contained in semi-purified endosomal fractions were increased in $CatS^{-/-}$ as compared with WT DCs (fig. S9, A and B). Hence, retention of Ii in endolysosomes of CatS-deficient DCs promotes the association of myosin II to these compartments.

When phosphorylated on Thr^{18} and/or Ser^{19}, MLC binds to and triggers the adenosine triphosphatase (ATPase) activity of the motor, initiating actomyosin contraction (*18*). To assess whether myosin II retention in endolysosomes from $CatS^{-/-}$ DCs decreases its activity, we analyzed the phosphorylation of MLC. Phosphorylation of the full-length 20-kD MLC was considerably decreased in $CatS^{-/-}$ cells compared with WT (Fig. 4, C and D). We consistently observed a 12-kD fragment of MLC that was verified by mass spectrometry in extracts from $CatS^{-/-}$ DCs (Fig. 4C and fig. S9, B and C). However, this MLC fragment did not react with the antiphosphorylated MLC antibody (Ab) (Fig. 4C), suggesting that it is inactive. Inhibition of CatS activity with LHVS triggered the accumulation of this 12-kD MLC fragment in WT but not in $Ii^{-/-}$ DCs (fig. S9D). Hence, retention of Ii in CatS-deficient DCs induces the specific accumulation of a truncated form of MLC. Thus, accumulation of Ii in DCs lacking CatS affects the subcellular localization and the activity of myosin II, providing a possible mechanism for regulation of DC motility by Ii.

We next investigated whether regulation of Ii expression upon DC activation leads to modification of their migratory capacity. Indeed, DCs undergo a transient increase in Ii and MHCII biosynthesis in the first hour after LPS treatment (*4*, *19*). Accordingly, although Ii-myosin II association was observed in nonactivated DCs, it was further increased after 1 hour of LPS treatment (fig. S10, A and B). We found that WT DCs activated with LPS for 2 hours exhibited strong alterations in their ability to migrate along microchannels (movie S6). Early activated WT DCs displayed significantly reduced instantaneous velocities (fig. S10D) and more fluctuant velocities and changed direction more frequently than untreated DCs (Fig. 4, E and F, and fig. S10C). The effect of LPS on motility was less marked in DCs treated with LPS for 12 hours, which moved slightly slower but with a similar persistence than nonactivated DCs (Fig. 4, E and F). LPS had no significant effect on the velocity and directionality of Ii-deficient DCs (Fig. 4, E and F, fig. S10D, and movie S7). Thus, the motility of DCs is regulated upon activation, and such regulation relies at least in part on Ii.

We show that Ii acts as a brake during DC motion by imposing a discontinuous locomotion mode that alternates between high and low motility phases. Down-modulation of cell migration by Ii is likely to result from its direct or

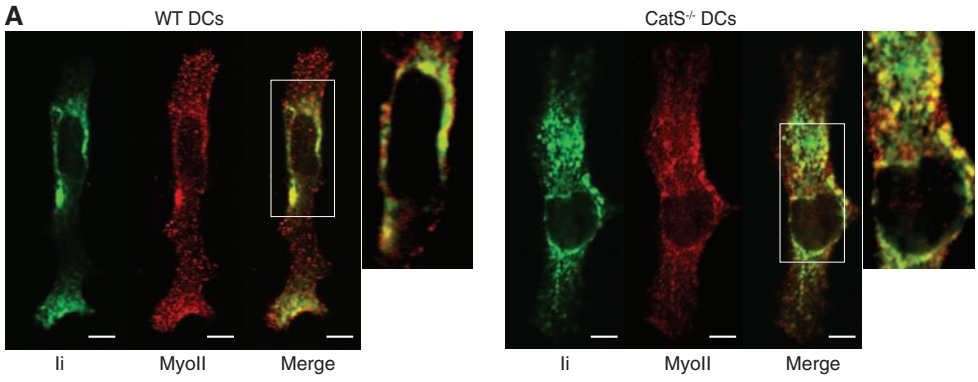

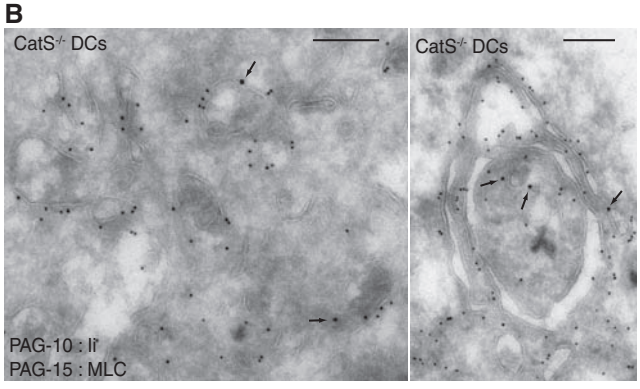

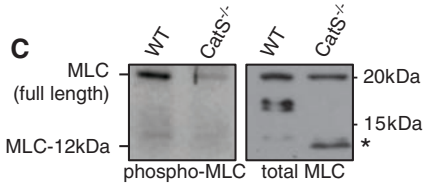

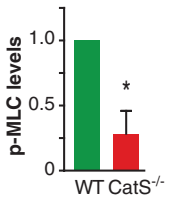

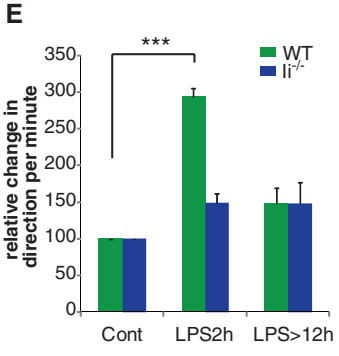

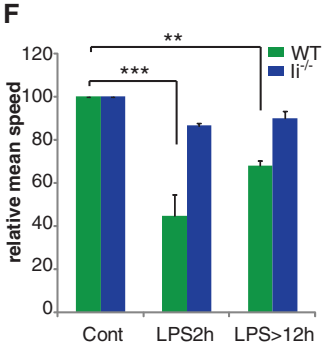

Fig. 4. The levels of Ii modify the localization and phosphorylation of myosin II as well as DC motility. (**A**) Immunofluorescence and confocal microscopy analysis of MyoIIHC and Ii subcellular localization in WT and CatS$^{-/-}$ BM-DCs plated on fibronectin-coated micropatterns. Scale bar, 2 μm. (**B**) Cryoimmunoelectron microscopy of CatS$^{-/-}$ BM-DCs. The colocalization of Ii and MLC was analyzed with secondary Abs coupled to protein A–gold (PAG) of 15-nm and 10-nm diameters, respectively. Scale bar, 200 nm (left) and 500 nm (right). (**C**) WT and CatS$^{-/-}$ DCs were lysed and analyzed by SDS–polyacrylamide gel electrophoresis and immunoblotting using antiphospho-MLC and antitotal MLC Abs sequentially. (**D**) MLC phosphorylation immunoblots were quantified by using Image J software; results were normalized to actin or tubulin expression and expressed as percentage of MLC phosphorylation in WT DCs (mean ± SD, three independent experiments, $*P = 0.01$). (**E** and **F**) The motility of LPS-pretreated cells along microchannels was analyzed by time-lapse imaging. Data are displayed as (E) the frequency of direction changes per minute and (F) the mean velocities, calculated by averaging instantaneous cell velocity values while taking into account cell directionality. Values are normalized to the ones of untreated cells from the same type (mean ± SD, 100 to 200 cells per condition from two independent experiments, $**P < 0.01$, $***P < 0.0001$).

indirect association with myosin II, which is required for polarized transport of MHCII-Ii complexes to endosomes in B cells (*7*). Ii–myosin II interaction would facilitate the convergence between MHCII and the endocytosed Ag but would temporarily affect the ability of myosin II to promote cell migration, thus leading to a transient decrease in DC velocity. Once in endosomes, Ii–myosin II complexes would dissociate upon Ii cleavage by CatS, restoring high DC motility.

The use of common regulators for Ag processing and cell motility provides a way for DCs to coordinate these two functions in time and space. In immature DCs that patrol peripheral tissues, the periodic low motility phases induced by Ii may enable DCs to efficiently couple Ag uptake and processing to cell migration, facilitating the sampling of the microenvironment. In early-activated DCs, the transient increase in the synthesis and association of Ii with myosin II would reduce the speed and confine the trajectories of the cells by promoting directional changes, enabling DCs to maximize Ag uptake (*2*). The formation of endocytic vesicles at the front of migrating DCs occurred within defined motility phases, suggesting a possible coupling between macropinocytosis and cell locomotion.

The physiological relevance of myosin II–dependent migration in DCs and other leukocytes was recently demonstrated (*6*). The molecular mechanism used by DCs to regulate their migratory capacity via myosin II is likely also used by B lymphocytes, in which myosin II and Ii associate upon B cell receptor engagement (*7*). Indeed, similarly to DCs, activated B cells from Ii$^{-/-}$ mice display enhanced motility ex vivo (fig. S11, A and B). Because myosin II was also shown to respond to Ag receptors in T and natural killer cells (*20*–*22*), we foresee that modulation of myosin II activity might be a general mechanism used by leukocytes to regulate their specific immune function in time and space.

References and Notes

1. J. A. Villadangos, P. Schnorrer, N. S. Wilson, *Immunol. Rev.* **207**, 191 (2005).
2. M. A. West *et al.*, *Science* **305**, 1153 (2004).
3. P. Pierre *et al.*, *Nature* **388**, 787 (1997).
4. M. Cella, A. Engering, V. Pinet, J. Pieters, A. Lanzavecchia, *Nature* **388**, 782 (1997).
5. J. Fink *et al.*, *Lab Chip* **7**, 672 (2007).
6. T. Lammermann *et al.*, *Nature* **453**, 51 (2008).
7. F. Vascotto *et al.*, *J. Cell Biol.* **176**, 1007 (2007).
8. M. F. Naujokas, M. Morin, M. S. Anderson, M. Peterson, J. Miller, *Cell* **74**, 257 (1993).
9. X. Shi *et al.*, *Immunity* **25**, 595 (2006).
10. G. P. Shi *et al.*, *Immunity* **10**, 197 (1999).
11. T. Y. Nakagawa *et al.*, *Immunity* **10**, 207 (1999).
12. C. Driessen *et al.*, *J. Cell Biol.* **147**, 775 (1999).
13. R. J. Riese *et al.*, *J. Clin. Investig.* **101**, 2351 (1998).
14. S. H. Chao, R. Carlson, D. R. Meldrum, *Lab Chip* **7**, 641 (2007).
15. D. Irimia, G. Charras, N. Agrawal, T. Mitchison, M. Toner, *Lab Chip* **7**, 1783 (2007).

16. Microchannels enable cell confinement during motion and therefore mimic the microenvironment encountered by DCs in the constrained interstitial spaces of peripheral tissues and lymphoid organs. They impose a directional migration to cells, which facilitates the extraction of measurable parameters. DCs entered and moved spontaneously and bidirectionally along microchannels, with their cell body being constrained during motion (fig. S4). Time-lapse movies obtained with WT, $Ii^{-/-}$, and $CatS^{-/-}$ DCs were analyzed by drawing kymographs and extracting cell positioning and instantaneous velocity data for individual migrating cells with a specialized computer program (figs. S4 and S5).
17. M. Boes *et al*., *Eur. J. Immunol.* **35**, 2552 (2005).
18. K. Clark, M. Langeslag, C. G. Figdor, F. N. van Leeuwen, *Trends Cell Biol.* **17**, 178 (2007).
19. J. A. Villadangos *et al*., *Immunity* **14**, 739 (2001).
20. J. Jacobelli, S. A. Chmura, D. B. Buxton, M. M. Davis, M. F. Krummel, *Nat. Immunol.* **5**, 531 (2004).
21. M. M. Andzelm, X. Chen, K. Krzewski, J. S. Orange, J. L. Strominger, *J. Exp. Med.* **204**, 2285 (2007).
22. K. Krzewski, X. Chen, J. S. Orange, J. L. Strominger, *J. Cell Biol.* **173**, 121 (2006).
23. The authors thank T. Makushok for setting up the cell migration microchannel system; A. Azicune for cell micropatterning techniques; W. Faigle and D. Lowe for proteomics analysis; C. Recchi for help with gelatin-FITC degradation experiments; H. Overkleeft for synthesizing the LHVS; J. Roger for providing magnetic nanoparticles; M. Leberre, D. Baigl, and Y. Chen for help with microfabrication; and S. Amigorena, M. Sixt, P. Benaroch, V. Soumelis, C. Hivroz, and I. Fernandez for advice on the manuscript. A.-M.L.-D. thanks Y. Bellaïche for help with manuscript redaction. G.F.-A. was supported by a fellowship from the Ministère Français de la Recherche and, together with M.H., from the Association pour la Recherche contre le Cancer (ARC). P.V. and M.-I.Y. benefited from ECOS–Comisíon Nacional de Investigacíon Científica y Technológica, Gobierno de Chile fellowship (CO3S01), Institut Curie and Inserm fellowships, respectively. V.S. was part of the Leonardo Da Vinci project (Unipharma-Graduates, Sapienza University of Rome). This work was funded in part by grants from the ARC, Fondecyt (Chile) to M.-R.B. (1060834) and M.R. (1060253); Agence Nationale pour la Recherche (ANR-06-PCVI-0010) and Human Frontiers Science Program (RGY53/2007) to M.P.

Supporting Online Material

www.sciencemag.org/cgi/content/full/322/5908/1705/DC1
Materials and Methods
Figs. S1 to S11
References
Movies S1 to S7

1 May 2008; accepted 27 October 2008
10.1126/science.1159894

A Role for the ESCRT System in Cell Division in Archaea

Rachel Y. Samson,[1]* Takayuki Obita,[2] Stefan M. Freund,[3] Roger L. Williams,[2] Stephen D. Bell[1]*†

Archaea are prokaryotic organisms that lack endomembrane structures. However, a number of hyperthermophilic members of the Kingdom *Crenarchaea*, including members of the *Sulfolobus* genus, encode homologs of the eukaryotic endosomal sorting system components Vps4 and ESCRT-III (endosomal sorting complex required for transport–III). We found that *Sulfolobus* ESCRT-III and Vps4 homologs underwent regulation of their expression during the cell cycle. The proteins interacted and we established the structural basis of this interaction. Furthermore, these proteins specifically localized to the mid-cell during cell division. Overexpression of a catalytically inactive mutant Vps4 in *Sulfolobus* resulted in the accumulation of enlarged cells, indicative of failed cell division. Thus, the archaeal ESCRT system plays a key role in cell division.

Within the archaeal domain of life, there are two principal Kingdoms, the *Crenarchaea* and the *Euryarchaea*. Studies of microbial diversity have revealed that crenarchaea are one of the most abundant forms of life on Earth (*1*, *2*); however, we know essentially nothing about how cell division occurs in these organisms. This is of particular interest because the sequenced genomes of hyperthermophilic crenarchaeotes lack genes for members of the FtsZ/tubulin and MreB/actin superfamilies of cell division proteins (*3*–*6*). The near-ubiquity of tubulins and actins underscores these proteins' pivotal roles in cell division processes in bacteria, euryarchaea, and eukarya. The absence of orthologs of these proteins in the crenarchaea has prompted us to attempt to identify the crenarchaeal cell division machinery, using species of the genus *Suflolobus* as a model system. In metazoa, the ESCRT (endosomal sorting complex required for transport) system, in addition to its roles in endosomal trafficking and viral egress (*7*–*10*), plays a role in membrane abscission during cytokinesis (*11*–*13*). Most hyperthermophilic crenarchaea encode homologs of ESCRT-III components and the adenosine triphosphatase (ATPase) Vps4 (*14*, *15*) that could potentially be involved in cell division (figs. S1 to S3). *Sulfolobus* encodes four ESCRT-III homologs and a single Vps4 homolog. No homologs of the ESCRT-0, -I, or -II systems are apparent. The Vps4 gene is located within an operon-like structure with an ESCRT-III homolog and a third protein predicted to contain a coiled-coil structure (fig. S1).

First, we profiled the cell-cycle expression of the *Sulfolobus* ESCRT machinery in synchronized cultures of *Sulfolobus acidocaldarius* (*16*, *17*) (Fig. 1, A and B). Transcripts of Saci1372 (Vps4) and ESCRT-III homologs Saci1373, -0451, and -1416 underwent a characteristic modulation, with lowest levels in S phase–enriched populations (at the 30-min time point) and levels peaking between three and four times higher in populations enriched in dividing cells (at 180 min). In agreement with this result, levels of Saci1373 (ESCRT-III) protein were highest in dividing cell populations (Fig. 1C, upper panel). In contrast, Vps4 protein remained nearly constant across the cell cycle (Fig. 1C, middle panel). Immunostaining with antibodies to Saci1373 (ESCRT-III) revealed a distinct subcellular localization of the protein. More specifically, in cells where the two nucleoids had separated, a band or belt of Saci1373 (ESCRT-III) was detected between the two nucleoids, correlating with the site of membrane ingression (Fig. 2, figs. S5 and S6, and movie S1). Similar results were observed for Vps4 localization, although in addition to the strong staining at mid-cell, we generally observed a weaker, diffuse background distributed throughout the cell body (Fig. 2). The highly specific localization of these proteins to the mid-cell in dividing cells suggested a role in cell division–related processes.

In eukaryotes, ESCRT-III family proteins are capable of both homo- and heteromultimeric interactions resulting in the generation of protein lattices. We tested the ability of the four *Sulfolobus* ESCRT-III homologs to interact with one another using yeast two-hybrid assays (Fig. 3A). A series of interactions between these proteins was detected, indicating that the archaeal ESCRT-III proteins have the capacity to form an extended lattice. In eukaryotes, Vps4 plays a pivotal role in disassembling the ESCRT-III lattice and has been shown to interact with ESCRT-III proteins via the MIT domain of Vps4 and the C-terminal tails of ESCRT-IIIs. We tested whether the Saci1373 (ESCRT-III) and Vps4 proteins interact directly. Full-length (residues 1 to 261) Saci1373 (ESCRT-III) and Saci1372 (Vps4) did indeed interact (Fig. 3, B and C). The minimal interaction sites comprised residues 183 to 193 of Saci1373 (ESCRT-III), a notably hydrophobic and proline-rich region (Fig. 3B), and the MIT domain of Saci1372 (Vps4) (Fig. 3C). To better understand the basis of this interaction, we determined the co-crystal structure of the MIT domain of Saci1372 (Vps4) with a peptide corresponding to residues 183 to 193 of Saci1373 (ESCRT-III). The MIT domain forms a three-helix bundle, and the peptide binds in an extended configuration to the groove formed between helices α1 and α3 (Fig. 3D). The residues interacting with the MIT domain constitute part of a 183-(R/K)XLLP(D/E)LPXPP-193 motif (*18*) present in most orthologs of Saci1373. Among the four Saci ESCRT-III–like subunits, only Saci1373

[1]Medical Research Council (MRC) Cancer Cell Unit, Hills Road, Cambridge CB2 0XZ, UK. [2]MRC Laboratory of Molecular Biology, Hills Road, Cambridge, CB2 0QH, UK. [3]MRC Centre for Protein Engineering, Hills Road, Cambridge CB2 0QH, UK.
*Present address: Sir William Dunn School of Pathology, South Parks Road, Oxford, OX1 3RE, UK.
†To whom correspondence should be addressed. E-mail: stephen.bell@path.ox.ac.uk